

# Collapse dynamics of super-Gaussian beams

Taylor D. Grow, Amiel A. Ishaaya, Luat T. Vuong and Alexander L. Gaeta

*School of Applied and Engineering Physics, Cornell University, Ithaca, NY 14853*

[a.gaeta@cornell.edu](mailto:a.gaeta@cornell.edu)

Nir Gavish and Gadi Fibich

*School of Mathematical Sciences, Tel Aviv University, Tel Aviv 69978, Israel*

**Abstract:** We investigate the self-focusing dynamics of super-Gaussian optical beams in a Kerr medium. We find that up to several times the critical power for self-focusing, super-Gaussian beams evolve towards a Townes profile. At higher powers the super-Gaussian beams form rings which break into filaments as a result of noise. Our results are consistent with the observed self-focusing dynamics of femtosecond laser pulses in air [1] in which filaments are formed along a ring about the axis of the initial beam where the initial beam did not form a ring.

© 2006 Optical Society of America

**OCIS codes:** (190.5530) Pulse propagation and solitons; (320.7110) Ultrafast nonlinear optics.

---

## References and links

1. J. Kasparian, M. Rodriguez, G. Méjean, J. Yu, E. Salmon, H. Wille, R. Bourayou, S. Frey, Y.-B. André, A. Mysyrowicz, R. Sauerbrey, J.-P. Wolf, and L. Wöste, "White-light filaments for atmospheric analysis," *Science* **301**, 61-64 (2003).
2. P. L. Kelley, "Self-focusing of optical beams," *Phys. Rev. Lett.* **15**, 1005-1008 (1965).
3. B. W. Zeff, B. Kleber, J. Fineberg, and D. P. Lathrop, "Singularity dynamics in curvature collapse and jet eruption on a fluid surface," *Nature (London)* **403**, 401-404 (2000).
4. P. A. Robinson, "Nonlinear wave collapse and strong turbulence," *Rev. Mod. Phys.* **69**, 507-573 (1997).
5. C. A. Sackett, J. M. Gerton, M. Welling, and R. G. Hulet, "Measurements of collective collapse in a Bose-Einstein condensate with attractive interactions," *Phys. Rev. Lett.* **82**, 876-879 (1999).
6. L. Bergé, S. Skupin, F. Lederer, G. Méjean, J. Yu, J. Kasparian, E. Salmon, J. P. Wolf, M. Rodriguez, L. Wöste, R. Bourayou, and R. Sauerbrey, "Multiple filamentation of terawatt laser pulses in air," *Phys. Rev. Lett.* **92**, 225002 1-4 (2004).
7. G. Fibich and A. L. Gaeta, "On the critical power for self-focusing in bulk media and hollow waveguides," *Opt. Lett.* **25**, 335-337 (2000).
8. G. Fraiman, "Asymptotic stability of manifold of self-similar solutions in self-focusing," *Sov. Phys. JETP* **61**, 228-233 (1985).
9. M. Landman, G. Papanicolaou, C. Sulem, and P. Sulem, "Rate of blowup for solutions of the nonlinear Schrödinger equation at critical dimension," *Phys. Rev. A* **38**, 3837-3843 (1988).
10. B. LeMesurier, P. Papanicolaou, C. Sulem, and P. Sulem, "Local structure of the self-focusing singularity of the nonlinear Schrödinger equation," *Physica D* **32**, 210-226 (1988).
11. F. Merle, and P. Raphael, "Sharp upper bound on the blow-up rate for the critical nonlinear Schrödinger equation," *Geom. Funct. Anal.* **13**, 591-642 (2003).
12. K. D. Moll, A. L. Gaeta, and G. Fibich, "Self-similar optical wave collapse: observation of the Townes profile," *Phys. Rev. Lett.* **90**, 203902 1-4 (2003).
13. G. Fibich, Nir Gavish, and Xiao-Ping Wang, "New singular solutions of the nonlinear Schrödinger equation," *Physica D* **211**, 193-220 (2005).
14. D. V. Skryabin and W. J. Firth, "Dynamics of self-trapped beams with phase dislocation in saturable Kerr and quadratic nonlinear media," *Phys. Rev. E* **58**, 3916-3930 (1998).

15. L. T. Vuong, T. D. Grow, A. Ishaaya, A.L. Gaeta, G. W. Hooft, E. R. Eliel, and G. Fibich, "Collapse of optical vortices," *Phys. Rev. Lett.* **96**, 133901 1-4 (2006).
16. A. J. Campillo, S. L. Shapiro and B. R. Suydam, "Periodic breakup of optical beams due to self-focusing," *Appl. Phys. B* **23**, 628-630 (1973).
17. J. M. Soto-Crespo, D. R. Heatley, and E. M. Wright, "Stability of the higher-bound states in a saturable self-focusing medium," *Phys. Rev. A* **44**, 636-644 (1991).
18. M. D. Feit and J. A. Fleck, Jr., "Beam nonparaxiality, filament formation, and beam breakup in the self-focusing of optical beams," *J. Opt. Soc. Am. B* **5**, 633-640 (1988).
19. J.M. Soto-Crespo, E.M. Wright and N.N. Akhmediev, "Recurrence and azimuthal-symmetry breaking of a cylindrical Gaussian beam in a saturable self-focusing medium," *Phys. Rev. A* **45**, 3168-3174 (1992).
20. V. I. Bespalov and V. I. Talanov, "Filamentary structure of light beams in non-linear liquids," *JETP Lett.* **3**, 307-310 (1966).
21. A. J. Campillo, S. L. Shapiro, B. R. Suydam, "Relationship of self-focusing to spatial instability modes," *Appl. Phys. Lett.* **24**, 178-180 (1974).
22. G. Fibich, S. Eisenmann, B. Ilan, Y. Erlich, M. Fraenkel, Z. Henis, A. L. Gaeta, and A. Zigler, "Self-focusing distances of very high power laser pulses," *Opt. Express* **13**, 5897-5903 (2005).
23. S. Skupin, L. Bergé, U. Peschel, F. Lederer, G. Méjean, J. Yu, J. Kasparian, E. Salmon, J. P. Wolf, M. Rodriguez, L. Wöste, R. Bourayou, and R. Sauerbrey, "Filamentation of femtosecond light pulses in the air: Turbulent cells versus long-range clusters," *Phys. Rev. E* **70**, 046602 1-15 (2004).
24. R. Y. Chiao, E. Garmire, and C. Townes, "Self-trapping of optical beams," *Phys. Rev. Lett.* **13**, 479-482 (1964).
25. L. Bergé, C. Gouédard, J. Schjodt-Eriksen, and H. Ward, "Filamentation patterns in Kerr media vs. beam shape robustness, nonlinear saturation and polarization states," *Physica D* **176**, 181-211 (2003).
26. A. Dubietis, E. Gaižauskas, G. Tamošauskas, and P. D. Trapani, "Light filaments without self-channeling," *Phys. Rev. Lett.* **92**, 253903 1-4 (2004).
27. A. L. Gaeta, "Catastrophic collapse of ultrashort pulses," *Phys. Rev. Lett.* **84**, 3582-3585 (2000).
28. G. Méchain, A. Couairon, Y.-B. André, C. D'Amico, M. Franco, B. Prade, S. Tzortzakakis, and A. Mysyrowicz, R. Sauerbrey, "Long-range self-channeling of infrared laser pulses in air: a new propagation regime without ionization," *Appl. Phys. B* **79**, 379-382 (2004).

Nonlinear wave collapse is universal to many areas of physics including optics [2], hydrodynamics [3], plasma physics [4], and Bose-Einstein condensates [5]. In optics, applications such as LIDAR and remote sensing in the atmosphere with femtosecond pulses depend critically on the collapse dynamics [1, 6]. The fundamental model for an optical beam propagating in a bulk medium with an intensity-dependent refractive index is described by the two-dimensional (2D) nonlinear Schrödinger equation (NLSE), and for powers above a certain critical power ( $P_{cr}$ ) the beam will undergo collapse until higher-order processes such as plasma generation halt the collapse [7]. Extensive theoretical analysis has shown that the beam collapses with a self-similar profile, known as the Townes profile (TP), at a square root rate with a log-log correction (the log-log law) [8–11]. Recent experiments confirmed that as a Gaussian beam approaches the point of collapse; the beam evolves to the TP [12]. Since the TP was observed independent of the initial noise or ellipticity of the beam, it was assumed that the TP was the only attractor for the 2D NLSE. However, recent theoretical work [13] has shown that super-Gaussian (SG) beams of sufficiently high power collapse towards a self-similar ring-shaped profile called the  $G$ -profile.

Ring-shaped profiles have been studied for a variety of conditions in nonlinear optics. Vortex beams, which are ring-shaped profiles with helical phase, have been shown theoretically to break apart into filaments at high power due to asymmetric phase [14] and the filamentation of vortex beams recently has been observed experimentally [15]. Another example of a ring-shaped beam is a beam with uniform phase that forms a ring due to diffraction, and at high powers these beams undergo filamentation due to modulational instability [16]. For any ring-shaped beam above the critical power, azimuthal filamentation is well-known [17–19].

In this paper, we experimentally examine the collapse dynamics of uniform-phase SG beams in which the ring profile is not present on the initial beam but is formed as the beam undergoes nonlinear propagation towards collapse. At low powers above  $P_{cr}$ , SG input beams behave similar to Gaussian profiles and collapse towards the self-similar TP. However, at higher powers,

a distinct behavior emerges for SG profiles in which the beam evolves to a ring profile and, in the presence of noise, undergoes multiple filamentation at much lower powers ( $P \sim 10P_{cr}$ ) than with a Gaussian beam ( $P \gtrsim 100P_{cr}$  [20–23]). Our experimental results are in excellent agreement with these predictions and provide clear quantitative evidence that the collapse dynamics of SG beams are fundamentally different from other input profiles previously studied.

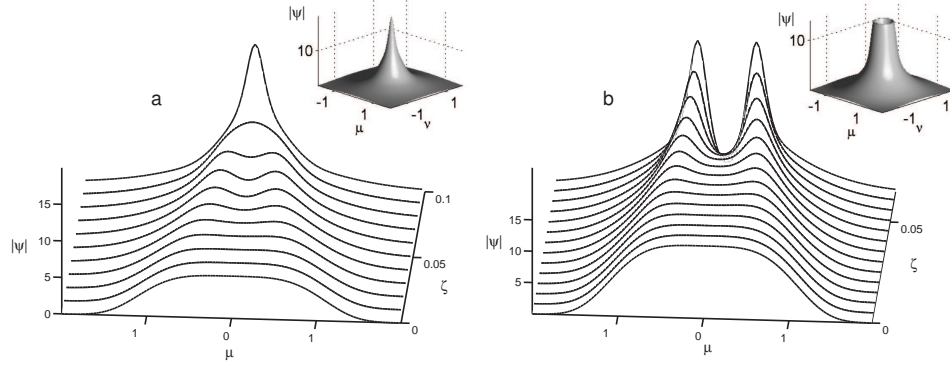


Fig. 1. Profiles of the solutions to the NLSE for a super-Gaussian input beam at two powers for various propagation distances  $\zeta$ . (a)  $P = 5P_{cr}$ , the beam collapses towards the Townes profile, (inset) three-dimensional plot for  $\zeta = 0.1$ . (b)  $P = 10P_{cr}$ , the beam forms a ring shape, (inset) three-dimensional plot for  $\zeta = 0.065$ .

The propagation of the beam in a Kerr medium is described by the dimensionless (2+1)D NLSE as

$$i\psi_{\zeta} + \nabla_{\perp}^2 \psi + |\psi|^2 \psi = 0, \quad (1)$$

where  $\psi(\nu, \mu, \zeta) = (r_0^2 k^2 n_2 c^3 / \pi)^{1/2} A(x, y, z)$ ,  $A$  is the amplitude of the envelope of the electric field,  $\zeta = z/2L_{df}$ ,  $\mu = x/r_0$ ,  $\nu = y/r_0$ ,  $\nabla_{\perp}^2$  is the transverse Laplacian, and  $L_{df} = kr_0^2$  is the diffraction length,  $r_0$  is the characteristic radius of the input beam,  $k = 2\pi n_0/\lambda$  is the wave number,  $\lambda$  is the vacuum wavelength,  $n_0$  is the linear index of refraction, and  $n_2$  is the nonlinear index coefficient. The last term of the left hand side of Eq. (1) gives rise to self-focusing as a result of the intensity-dependent refractive index  $n = n_0 + n_2 I$ , where  $I$  is the intensity. The precise threshold for self-focusing depends upon the profile of the input beam [7]. In this paper, we define  $P_{cr}$  to be the critical power for a Gaussian input beam.

Numerical integration of Eq. (1) for an initial beam with a uniform-phase SG field distribution at two different input powers is shown in Fig. 1. For an input beam of  $5P_{cr}$  the SG beam collapses towards the TP similar to the observed behavior for a Gaussian beam [24]. However a SG beam with  $10P_{cr}$  does not evolve to the TP but forms a ring shape. The initial formation of the ring can be understood by the following argument. For  $P \gg P_{cr}$  the nonlinearity dominates over diffraction, and the NLSE is approximated by

$$i\psi_{\zeta} + |\psi|^2 \psi = 0. \quad (2)$$

The solution of Eq. (2) is given by

$$\psi = \psi_0(\mu, \nu) e^{ik_0 S}, \quad (3)$$

where

$$S(\rho, \zeta) = \frac{2n_2}{n_0} |\psi_0|^2 \zeta. \quad (4)$$

We recall that the transformation from the nonlinear Helmholtz equation (NLHE) to the NLSE was done via the substitution  $E = e^{ik_0\zeta}\psi$ . Thus, if we look for a solution of the NLHE of the form

$$E(\rho, \zeta) = A_H(\rho, \zeta)e^{ik_0S_H}, \quad (5)$$

then  $S_H = (1 + (2n_2/n_0)|\psi_0|^2)\zeta$ . In Fig. 2 we plot the phase fronts and rays for Gaussian and SG input beams. The flat-top phase profile of the SG beam acts as a lens to focus the rays into a ring-like structure in contrast to the Gaussian phase profile which focuses the rays towards the center. Thus, the initial ring formation can be understood to be a result of nonlinear propagation over distances in which diffraction is negligible.

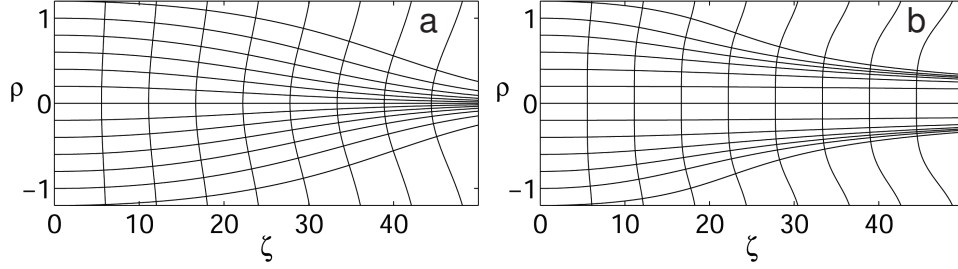


Fig. 2. Nonlinear propagation of rays (horizontal lines) and phase fronts (vertical lines) for (a) Gaussian ( $S_H = (1 + \frac{1}{9}e^{-\rho^2})\zeta$ ) and (b) super-Gaussian ( $S_H = (1 + \frac{1}{9}e^{-\rho^4})\zeta$ ) input beams.

After the initial ring formation, the beams will continue to collapse and Fibich et. al. [13] have shown that the collapse rate for SG beams is different than that for Gaussian beams, which collapse to the TP, and that the profile evolves to a ring-shaped self-similar profile called the  $G$ -profile [13]. In our numerical simulations the  $G$ -profile persists at extremely high intensities and does not form a TP as the beam collapses. Though it is necessary to confirm self-similarity of the  $G$ -profile by performing simulations up to intensities far beyond what is physically possible to observe, the drastic difference in dynamics for a SG beam compared to that of a Gaussian beam is still evident at intensities well within an observable regime (See Fig. 1). However, we find that the  $G$ -profile is unstable to non-radially symmetric noise (amplitude or phase) and eventually the beam breaks into filaments along the ring (an initial observation of a difference in multiple filamentation for a SG as compared to Gaussian input was first reported in [25]). We solve the NLSE for a SG input beam with several types of noise. For radially symmetric noise we observe the ring to be stable. However for noise without radial symmetry, the ring becomes unstable as shown in Fig. 3. We conducted similar simulations with SG beams that are slightly elliptical and find that the ring also breaks apart into filaments similar to those shown for a noisy profile in Fig. 3 but regularly spaced. This filamentation process occurs for SG profiles with noise as small as 1% and for input powers as low as  $10P_{cr}$ . From this we conclude that noise or asymmetry do not determine the transition from a centrosymmetric TP to a ring-shaped profile but do lead to the break up of the ring into filaments, as has been observed for other ring-shaped profiles. We also find that the amount of noise on the input profile changes the distance at which filamentation occurs but not the number of filaments.

The number of filaments into which the ring breaks can be predicted by following a similar azimuthal modulational instability analysis as that used to predict the number of filaments for collapsing vortex beams [15]. We assume the beam forms a uniform-phase ring,  $\psi(r) = (r/w)e^{-(r/w)^2}$ , and solve for the number of azimuthal maxima ( $\eta$ ) which yields

$$\eta = \sqrt{2e^{-1}(2Pw^2\alpha - e)}, \quad (6)$$

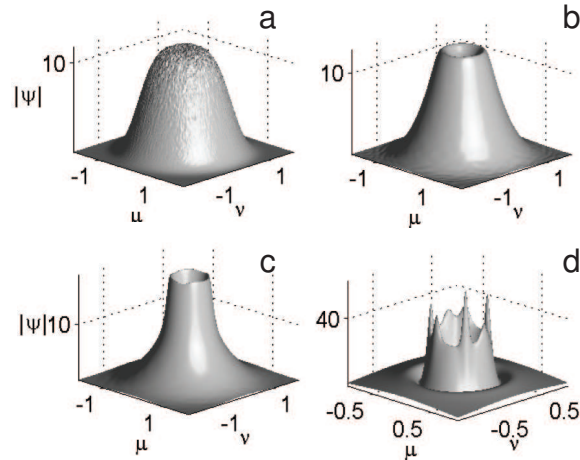


Fig. 3. Solutions to the NLSE with a super-Gaussian input beam with 5% amplitude noise (phase noise produces similar results) and an input power of  $20 P_{cr}$  at distances (a)  $\zeta = 0$ , (b)  $\zeta = 0.025$ , (c)  $\zeta = 0.0375$ , and (d)  $\zeta = 0.05$ .

where  $\alpha = 1.8962$  from [7] and  $w$  determines the radius of the ring. Different input powers of a SG beam will each produce a ring at a slightly different radius (see Fig. 4). We choose  $w = 0.7$  which produces a ring with a radius approximately equal to the rings observed in the simulations. Figure 4 shows the number of predicted filaments versus power from our analysis compared to the approximate number of filaments observed in the numerical simulations. The modulationally instability analysis assumes a uniform-phase SG input, and the numerical integration starts with an initial amplitude noise of 10 %. The close agreement between the predictions of the modulationally instability analysis and the numerical simulations show that the number of filaments formed by a SG beam is proportional to the square-root of the input power.

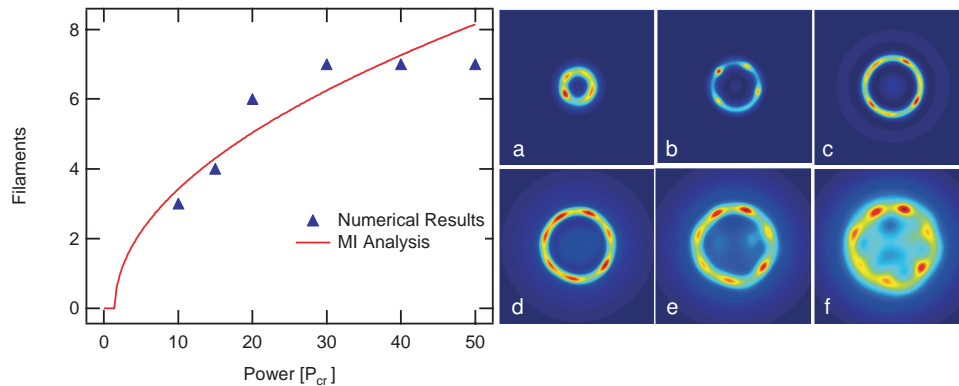


Fig. 4. Left: Comparison of our modulational instability analysis with the approximate number of filaments observed in the numerical simulations. Right: Numerically simulated filamentation of an initially super-Gaussian beam with 10% amplitude noise for input powers of (a)  $10 P_{cr}$ , (b)  $15 P_{cr}$ , (c)  $20 P_{cr}$ , (d)  $30 P_{cr}$ , (e)  $40 P_{cr}$ , (f)  $50 P_{cr}$ .

To experimentally investigate the collapse of SG beams, we used the setup shown in Fig. 5. A 90-fs, 800-nm pulse from a Ti:sapphire amplifier with a repetition rate of 1 kHz is sent through a

spatial filter and is reflected from a two-dimensional spatial light modulator (Hamamatsu PPM X8267). The spatial light modulator allows the amplitude of the input beam profile to be altered with a high degree of spatial control. The size of the beam is then reduced using a telescopic arrangement, and the spatial light modulator is imaged onto the input face of a deionized water cell. We record the input profile by removing the cell and imaging the input beam onto a 12-bit CCD camera (Spiricon LBA-FW-SCOR20). We then replace the cell and image the output face of the cell for different input parameters. In order to observe the dynamics of the pulse as it propagates through different lengths of the medium, the water cell is adjustable in length [26]. This setup is ideal for observing dynamics as it allows for fine control over the power, size, and shape of the input beam and over the length of the medium.

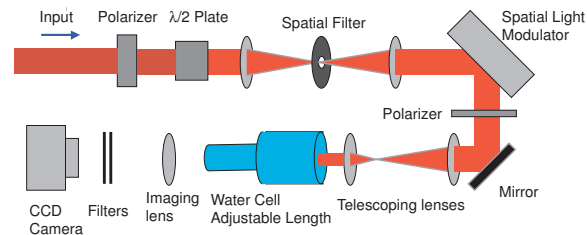


Fig. 5. Schematic of the experimental set up used to observe beam collapse. In the experiment the beam is reflected from the spatial light modulator at a near-normal incidence.

Figure 6 shows an experimental comparison of Gaussian versus SG collapse dynamics at high powers. For the case of a Gaussian input beam, the input is imaged in Fig. 6(a), and Fig. 6(b) shows the image of the output after traveling through the 7-cm length cell. The energy is increased until the point just below the threshold for super-continuum generation, which is a signature that the beam has undergone collapse [27]. The Gaussian input beam collapses to a TP, which is in agreement with previous experiments [12]. When the input profile is slightly altered to produce a more flat-topped profile [Fig. 6(c)], which approximates a SG, the profile no longer evolves to a TP but more closely resembles a broken ring [Fig. 6(d)] as predicted by our numerical simulations.

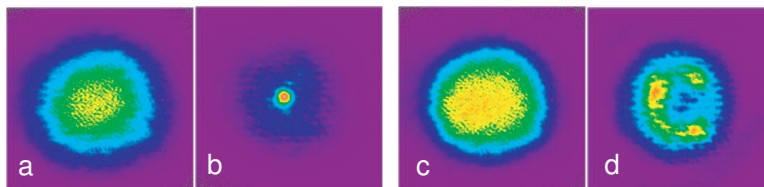


Fig. 6. Images of the input and output intensity beam profiles for a 7-cm propagation distance (0.9 mm X 0.9 mm). (a) Gaussian input profile, (b) output beam with the Gaussian input and an input energy of  $E = 5.6 \mu\text{J}$ , (c) super-Gaussian input profile, (d) output beam with a super-Gaussian input and an input energy of  $E = 5.0 \mu\text{J}$ . The pulse energies were just below the threshold for supercontinuum generation.

Figure 7 illustrates how a beam with a SG profile, evolves as it propagates through the medium. When the cell is set to 1.3 cm, a dip forms in the center. As the length of the cell is increased, the ring develops and then breaks into individual filaments as expected for beams with noise. We also tested ring-shaped input profiles and we observe similar filamentation of the ring as that shown for SG inputs. These results agree with our theoretical predictions that a noisy SG beam with sufficiently high power will form a ring of filaments. Similar rings of

filaments have been observed for high-power flat-top beams in air [28].

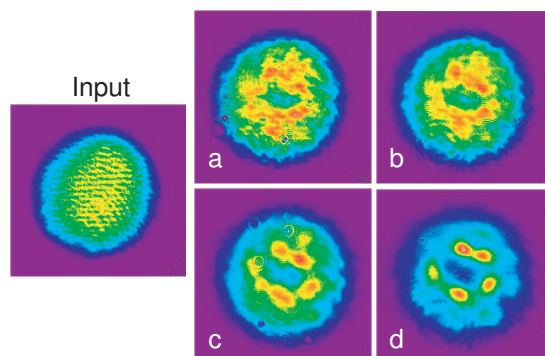


Fig. 7. Experimental intensity distributions of an initially super-Gaussian beam ( $E = 13.3 \mu\text{J}$ ) as it propagates in the water cell. The image area is  $0.3 \text{ mm} \times 0.3 \text{ mm}$ . Left: Input profile. Right: Output profiles with the length of the water cell set at, (a) 1.3 cm, (b) 2.0 cm, (c) 3.0 cm, and (d) 4.3 cm.

Figure 8 shows the dependence of SG collapse profiles as a function of input power for a 10-cm cell. A low-power SG [Fig. 8(a)] input collapses towards a TP [Fig. 8(d)]. In order to observe the dynamics at higher powers, the spatial light modulator was used to produce a SG with sequentially larger diameters in Fig. 8(b) and (c) for increasing input powers. This allows us to increase the power in the beam while avoiding super-continuum generation and minimizing dispersion effects present in a longer cell. The output profiles in Fig. 8(e) and (f) clearly show the transition of the TP to the ring of filaments as the power increases. We were not able to explore higher powers above those shown due to the potential of damaging the SLM. This is experimental confirmation that a low-power SG beam collapses towards the TP, while a higher power SG beam collapses to a ring that then breaks into filaments.

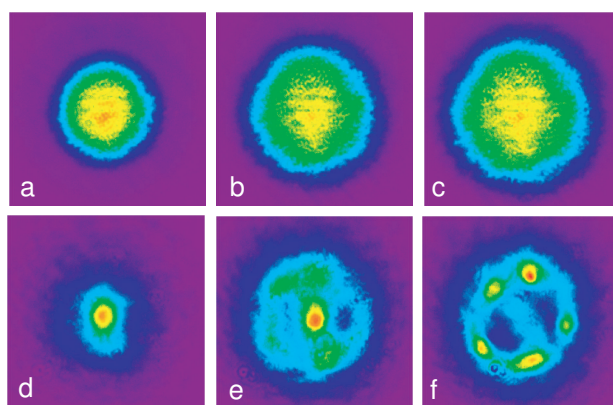


Fig. 8. Input super-Gaussian beams (a-c) for increasing energy and corresponding output profiles (d-f) just before the super-continuum threshold in a 10-cm cell. (d)  $E = 4.2 \mu\text{J}$ ,  $I = 3.3 \times 10^{10} \text{ W/cm}^2$ , (e)  $E = 9.1 \mu\text{J}$ ,  $I = 4.6 \times 10^{10} \text{ W/cm}^2$ , (f)  $E = 17.5 \mu\text{J}$ ,  $I = 6.2 \times 10^{10} \text{ W/cm}^2$ . The image area is  $1 \text{ mm} \times 1 \text{ mm}$ .

These results illustrate a new path to multiple filamentation that depends critically on changes

in the shape of the input beam. Typically multiple filamentation in the NLSE for a Gaussian input is not expected to occur unless the power is greater than  $100P_{cr}$  [22] due to modulational instability. Neglecting the effects of dispersion, the SG profiles in Fig. 6 and Fig. 7 have powers of  $31P_{cr}$  and  $83P_{cr}$ , respectively, which are both lower than the powers expected for filamentation with a Gaussian beam. In our simulations we observe similar behavior for powers as low as  $10P_{cr}$ .

In conclusion, we have experimentally confirmed that at high powers the SG collapse dynamics are fundamentally different than those of Gaussian beams. A SG with power a few times the critical power will collapse towards the TP similar to a Gaussian beam. At higher powers a noiseless SG beam will collapse towards a ring-shape that becomes the self-similar  $G$ -profile at extremely high intensities. With the addition of noise, the ring breaks apart into filaments. While collapse of other annular beams, such as uniform-phase doughnut and vortex beams may have shown similar filamented ring patterns, the transition from TP to filamented rings for a SG input is unique. These results offer a compelling explanation of the ring-shaped filamentation that occurs with very high power femtosecond pulses self-focusing in air [1]. Lastly, we expect that ring-type profiles could occur in Bose-Einstein condensates since their dynamics is also governed by the Gross-Pitaevskii equation which is similar to the NLSE.

This work is supported by the National Science Foundation under grant PHY-0244995 and the Army Research Office under Grant No. 48300-PH.